

Optimizing interferometer experiments for CMB B mode measurement

Jaiseung Kim^{1?}

¹ Dept. of Physics, Brown Univ. Providence, U.S.A.

ABSTRACT

The sensitivity of interferometers with linear polarizers to the CMB E and B mode are variant under the rotation of the polarizer frame, while interferometer with circular polarizers are equally sensitive to E and B mode. We present analytically and numerically that the diagonal elements of window functions for CMB E/B power spectra are maximized in interferometric measurement of linear polarization, when the polarizer frame is in certain rotation from the associated baseline. We also present the simulated observation to show that the 1- errors on E/B mode power spectrum estimation are variant under the polarizer frame rotation in the case of linear polarizers, while they are invariant in the case of circular polarizers. Simulation of the configuration similar to the DASI shows that minimum 1- error on B mode in interferometric measurement with linear polarizers is 26% of that in interferometric measurement with circular polarizers. The simulation also shows that the E/B mixing in interferometric measurement with linear polarizers can be as low as 23% of that in interferometric measurement with circular polarizers. It is not always possible to physically align the the polarizer frame with all the associated baselines in the case of an interferometer array ($N > 2$). There exist certain linear combinations of visibilities, which are equivalent to visibilities of the optimal polarizer frame rotation. We present the linear combinations, which enables B mode optimization for an interferometer array ($N > 2$).

Key words: { cosmology:cosmic microwave background { techniques:interferometric

1 INTRODUCTION

The Cosmic Microwave Background (CMB) is expected to be linearly polarized by Thomson scattering at the last scattering surface and after re-ionization. The detection of the CMB polarization has been reported by the Degree Angular Scale Interferometer (DASI) (Kovac et al. 2002) and recently by the Wilkinson Microwave Anisotropy Probe (WMAP) satellite (Page et al. 2006). Measurements of the CMB temperature anisotropy with interferometers are made in the Very Small Array (VSA), the Cosmic Background Imager (CBI) and many other experiments. The CMB polarization measurements with interferometers are on-going and planned in the experiments such as DASI, CBI and the Millimeter-wave Bolometric Interferometer (MBI) (Tucker et al. 2003; Kurotkov et al. 2006). With many desirable features of an interferometer, interferometers are more and more employed in CMB polarization experiments.

The CMB polarization can be decomposed into gradient-like E mode and curl-like B mode (Zaldarriaga and Seljak 1997). B mode polarization is

not induced by scalar density perturbation but only tensor perturbation, while E mode polarization is induced by both (Seljak and Zaldarriaga 1997). Since tensor-to-scalar ratio is much smaller than unity in most inflationary models, B mode polarization is expected to be much smaller than E mode polarization. Though there is complication by gravitational lensing (Okamoto and Hu 2003), measurement of B mode polarization makes it possible probing the universe on the energy scale at inflationary period (Dodson 2003).

The 1- error on the parameter estimation can be forecast from the Fisher matrix (Dodson 2003). It will be shown that in interferometric measurement of Stokes parameter Q or U, the 1- error on E and B power spectra estimation varies with rotation of its polarizer frame. We will show that certain rotation of the polarizer frame from the associated baseline minimize the 1- error on either E or B mode power spectra estimation. For a feedhorn array ($N > 2$), it is not always possible to realize the specific rotation of the polarizer frame from all the associated baselines. We will show that forming certain linear combinations of polarimetric visibilities is identical with physically rotating the polarizer frame to the optimal orientation, thereby enabling the B mode measurement optimization for a feedhorn array ($N > 2$).

? E-mail: jkim@physics.brown.edu

arXiv:astro-ph/0611564v3 22 Nov 2006

This paper is organized as follows. We discuss Stokes parameters in x2. The formalism for interferometric CMB polarization measurement on spherical sky is presented in x3. In x4, with flat sky approximation, we show that interferometric measurement of Stokes parameter Q or U can be configured to suppressing E mode, leading to smaller leakage between E and B mode. In x5, we discuss the variation of 1- error on power spectra estimation and show that B mode sensitivity is maximized, when the polarizer frame is in certain rotation from the baseline. In x6, we show that there exists certain linear combinations of visibilities, which enables the B mode optimization for a feedhorn array (N > 2). In x7, the summary and conclusion are given. In appendix, we show analytically that the diagonal element of window functions are maximized, when the polarizer frame is rotated from the baseline by certain angles.

2 STOKES PARAMETERS

There are Stokes parameters, which describe the state of polarization (Kraus 1986), which are measured in reference to $(\hat{e}; \hat{e})$ (Zaldarriaga and Seljak 1997). \hat{e} and \hat{e} are the unit vectors of the spherical coordinate system and given by (Arfken and Weber 2000)

$$\begin{aligned} \hat{e} &= \hat{i} \cos \theta \cos \phi + \hat{j} \cos \theta \sin \phi - \hat{k} \sin \theta; \\ \hat{e} &= -\hat{i} \sin \phi + \hat{j} \cos \phi; \end{aligned}$$

Since Thomson scattering does not generate circular polarization but linear polarization in early universe, the phase difference between E and E is zero and circular polarization state V is redundant in the study on the CMB polarization. Stokes parameters Q and U are as follows:

$$Q = E_x^2 - E_y^2; \quad (1)$$

$$U = 2E_x E_y i; \quad (2)$$

where $\langle \cdot \rangle$ indicates time average. Q and U transform under rotation of an angle α on the plane perpendicular to direction \hat{n} as

$$Q^0(\hat{n}) = Q(\hat{n}) \cos 2\alpha + U(\hat{n}) \sin 2\alpha; \quad (3)$$

$$U^0(\hat{n}) = -Q(\hat{n}) \sin 2\alpha + U(\hat{n}) \cos 2\alpha; \quad (4)$$

with which the following quantities can be constructed (Zaldarriaga and Seljak 1997):

$$Q^0(\hat{n}) - iU^0(\hat{n}) = e^{2i\alpha} (Q(\hat{n}) - iU(\hat{n})); \quad (5)$$

For all-sky analysis, Q and U are expanded in terms of spin-2 spherical harmonics (Zaldarriaga and Seljak 1997) as follows:

$$Q(\hat{n}) + iU(\hat{n}) = \sum_{l,m} (a_{E;l,m} + ia_{B;l,m}) {}_2Y_{lm}(\hat{n}); \quad (6)$$

$$Q(\hat{n}) - iU(\hat{n}) = \sum_{l,m} (a_{E;l,m} - ia_{B;l,m}) {}_2Y_{lm}(\hat{n}); \quad (7)$$

3 INTERFEROMETRIC MEASUREMENT

An interferometer measures time-averaged correlation of two electric field from a pair of identical apertures positioned at r_1 and at r_2 . The separation, $B = r_1 - r_2$, of two apertures is

called the 'baseline' and the measured value is called 'visibility' (Lawson 1999). Depending on the instrumental configuration, visibilities are associated with $\langle E_x^2 - E_y^2 \rangle$, $\langle 2E_x E_y i \rangle$ and $\langle E_x^2 + E_y^2 - 2E_x E_y i \rangle$ respectively, where \hat{x} and \hat{y} are axes of the polarizer frame. As discussed in x2, Stokes parameters at angular coordinate (θ, ϕ) are defined in respect to two basis vectors \hat{e} and \hat{e} . Consider the polarization observation, whose antenna pointing is in the direction of angular coordinate (θ_A, ϕ_A) . The polarizers and baselines are assumed to be on the aperture plane. Then, the polarizer frame is the system rotated by Euler angles (α, β, γ) , where α is the rotation around the axis in the direction of antenna pointing. Geometrical illustration for the relations between (\hat{e}, \hat{e}) , (\hat{e}_A, \hat{e}_A) and (\hat{e}_x, \hat{e}_y) are given in Fig. 1. Two basis vectors of the polarizer frame are as follows:

$$\begin{aligned} \hat{e}_x &= \hat{e}_A \cos \alpha + \hat{e}_A \sin \alpha; \\ \hat{e}_y &= -\hat{e}_A \sin \alpha + \hat{e}_A \cos \alpha; \end{aligned}$$

where

$$\begin{aligned} \hat{e}_A &= \hat{i} \cos \theta_A \cos \phi_A + \hat{j} \cos \theta_A \sin \phi_A - \hat{k} \sin \theta_A; \\ \hat{e}_A &= -\hat{i} \sin \phi_A + \hat{j} \cos \phi_A; \end{aligned}$$

Most of interferometer experiments for the CMB observation employ feedhorns to collect beam. In a feedhorn system, the basis vectors \hat{e} and \hat{e} of the ray are projected on the plane parallel to the aperture. Projected on the aperture plane, the basis vectors \hat{e} and \hat{e} of the ray are related to the basis vectors \hat{e}_x and \hat{e}_y as follows¹:

$$\hat{e}_x + i\hat{e}_y = e^{i\alpha} (\hat{e} + i\hat{e}); \quad (8)$$

where α is the azimuthal angle of the basis vector \hat{e} in the polarizer frame, given by

$$\tan^{-1} \frac{\hat{e}_y \cdot \hat{e}}{\hat{e}_x \cdot \hat{e}} = \alpha;$$

where

$$\begin{aligned} &= \tan^{-1} \frac{\hat{e} \cdot \hat{e}_A}{\hat{e} \cdot \hat{e}_A} \\ &= \tan^{-1} \frac{\cos \theta \sin(\phi - \phi_A)}{\cos \theta \cos \theta_A \cos(\phi - \phi_A) + \sin \theta \sin \theta_A}; \end{aligned}$$

With Eq. 8, we can easily show that

$$\langle E_x^2 - E_y^2 + i2E_x E_y i \rangle = e^{i(2\alpha - 2\alpha)} (\langle E^2 - E^2 + i2E E i \rangle);$$

With the employment of linear polarizers, the visibilities associated with $\langle E_x^2 - E_y^2 \rangle$ or $\langle 2E_x E_y i \rangle$ are as follows:

$$V_{Q0} = \int dA(\hat{n}, \hat{n}_A) \text{Re} [e^{i(2\alpha - 2\alpha)} (Q(\hat{n}) + iU(\hat{n}))] e^{i2\alpha} \hat{n}; \quad (9)$$

$$V_{U0} = \int dA(\hat{n}, \hat{n}_A) \text{Im} [e^{i(2\alpha - 2\alpha)} (Q(\hat{n}) + iU(\hat{n}))] e^{i2\alpha} \hat{n}; \quad (10)$$

¹ This relation is approximately valid, since the projected \hat{e} and \hat{e} are not orthogonal to each other. The approximation breaks down, when the primary beam is very large.

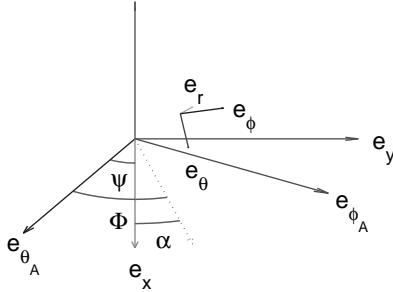


Figure 1. geometrical relations among $(\hat{e}_r, \hat{e}_\phi)$, (\hat{e}_A, \hat{e}_A) and (\hat{e}_x, \hat{e}_y)

where \hat{n}_A is the unit vector in the direction of antenna pointing and $f(\nu)$ is the frequency spectrum of the CMB polarization.²

With the employment of circular polarizers, the visibilities associated with $\hat{e}_x^2 - \hat{e}_y^2$ and $i\hat{e}_x\hat{e}_y$ are as follows:

$$V_{RL} = f(\nu) \int dA(\hat{n} \cdot \hat{n}_A) \quad (11)$$

$$[Q(\hat{n}) + iU(\hat{n})]e^{i(2\nu\hat{n} \cdot \hat{n}_A + 2\pi\hat{n} \cdot \hat{n}_A)};$$

$$V_{LR} = f(\nu) \int dA(\hat{n} \cdot \hat{n}_A) \quad (12)$$

$$[Q(\hat{n}) - iU(\hat{n})]e^{i(2\nu\hat{n} \cdot \hat{n}_A + 2\pi\hat{n} \cdot \hat{n}_A)};$$

where R and L stand for right/left circular polarizers.

With Eq. 6 and 7, visibilities are expressed in terms of E/B mode as follows:

$$V_{Q^0} = f(\nu) \int dA(\hat{n} \cdot \hat{n}_A) e^{i(2\nu\hat{n} \cdot \hat{n}_A)} \quad (13)$$

$$\text{Re} \int e^{i(2\pi\hat{n} \cdot \hat{n}_A)} (a_{E;l,m} + ia_{B;l,m}) {}_2Y_{lm};$$

$$V_{U^0} = f(\nu) \int dA(\hat{n} \cdot \hat{n}_A) e^{i(2\nu\hat{n} \cdot \hat{n}_A)} \quad (14)$$

$$\text{Im} \int e^{i(2\pi\hat{n} \cdot \hat{n}_A)} (a_{E;l,m} + ia_{B;l,m}) {}_2Y_{lm};$$

$$V_{RL} = f(\nu) \int dA(\hat{n} \cdot \hat{n}_A) \quad (15)$$

$$(a_{E;l,m} + ia_{B;l,m}) {}_2Y_{lm} e^{i(2\nu\hat{n} \cdot \hat{n}_A + 2\pi\hat{n} \cdot \hat{n}_A)};$$

$$V_{LR} = f(\nu) \int dA(\hat{n} \cdot \hat{n}_A) \quad (16)$$

$$(a_{E;l,m} - ia_{B;l,m}) {}_2Y_{lm} e^{i(2\nu\hat{n} \cdot \hat{n}_A + 2\pi\hat{n} \cdot \hat{n}_A)};$$

² $f(\nu) = \frac{\partial B(\nu; T)}{\partial T} \Big|_{T=T_0}$, where $B(\nu; T)$ is the Planck function and T_0 is the CMB monopole temperature.

4 REDUCING LEAKAGE BETWEEN E AND B MODE

For the observation of small patch of sky, at sky approximation in small angle limit can be used. In at sky approximation, Eq. 9, 10, 11 and 12 are as follows:

$$V_{Q^0} = f(\nu) \int dx^2 A(x) \text{Re} \int e^{2i\pi fQ(x) + iU(x)g} e^{i2\nu x};$$

$$V_{U^0} = f(\nu) \int dx^2 A(x) \text{Im} \int e^{2i\pi fQ(x) + iU(x)g} e^{i2\nu x};$$

$$V_{RL} = f(\nu) \int dx^2 A(x) [Q(x) + iU(x)] e^{i(2\nu x + 2\pi)};$$

$$V_{LR} = f(\nu) \int dx^2 A(x) [Q(x) - iU(x)] e^{i(2\nu x + 2\pi)};$$

where $A(x)$ is the function of beam power pattern. Since visibilities are the convolution of the Fourier transform of a beam function with the Fourier transform of Q and U (M. P. Hobson and M. Ainsinger 2002), they can be written as follows:

$$V_{Q^0} = f(\nu) \int d^2u^0 \tilde{A}(u - u^0) [\cos(2\pi) \tilde{Q}(u^0) + \sin(2\pi) \tilde{U}(u^0)];$$

$$V_{U^0} = f(\nu) \int d^2u^0 \tilde{A}(u - u^0) [\sin(2\pi) \tilde{Q}(u^0) + \cos(2\pi) \tilde{U}(u^0)];$$

$$V_{RL} = f(\nu) \int d^2u^0 \tilde{A}(u - u^0) e^{i2\pi} (\tilde{Q}(u^0) + i\tilde{U}(u^0));$$

$$V_{LR} = f(\nu) \int d^2u^0 \tilde{A}(u - u^0) e^{i2\pi} (\tilde{Q}(u^0) - i\tilde{U}(u^0));$$

where $\tilde{\sim}$ indicates Fourier transform. In the at sky approximation in small angle limit, Stokes parameter Q and U can be decomposed as follows (Zaldarriaga and Seljak 1997):

$$\tilde{Q}(u) = \cos(2\pi u) \tilde{E}(u) - \sin(2\pi u) \tilde{B}(u); \quad (17)$$

$$\tilde{U}(u) = \sin(2\pi u) \tilde{E}(u) + \cos(2\pi u) \tilde{B}(u); \quad (18)$$

where u is the direction angle of a vector u . With Eq. 17 and 18, visibilities are expressed in terms of E and B mode as follows:

$$V_{Q^0} = f(\nu) \int d^2u^0 \tilde{A}(u - u^0) [\cos(2\pi(u - u^0)) \tilde{E}(u^0) + \sin(2\pi(u - u^0)) \tilde{B}(u^0)]; \quad (19)$$

$$V_{U^0} = f(\nu) \int d^2u^0 \tilde{A}(u - u^0) [\sin(2\pi(u - u^0)) \tilde{E}(u^0) + \cos(2\pi(u - u^0)) \tilde{B}(u^0)]; \quad (20)$$

$$V_{RL} = f(\nu) \int d^2u^0 \tilde{A}(u - u^0) e^{i2\pi(u - u^0)} (\tilde{E}(u^0) + i\tilde{B}(u^0)); \quad (21)$$

$$V_{LR} = f(\nu) \int d^2u^0 \tilde{A}(u - u^0) e^{i2\pi(u - u^0)} (\tilde{E}(u^0) - i\tilde{B}(u^0)); \quad (22)$$

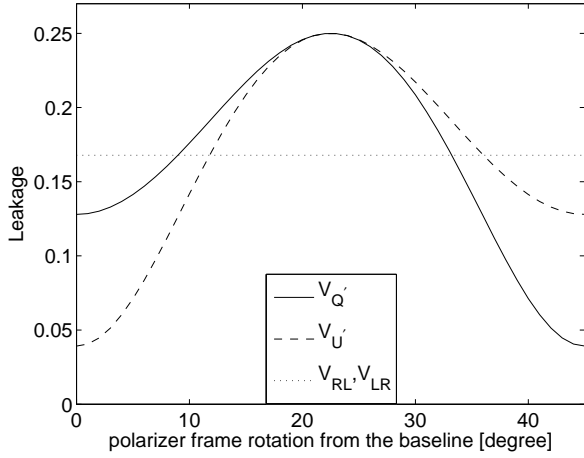


Figure 2. L_{EB} and L_{BE} for various ψ_u

A Gaussian beam is a good approximation to many CMB experiments and the Fourier transform of a Gaussian beam is $\exp[-\frac{j^2 u^2}{2}]$, where $\psi_u = 0.4245 \text{ FWHM}$. With such a beam, biggest contribution comes from $u^0 = u$ in the integration over u^0 . We can approximate visibilities as follows:

$$V_{Q^0} = f(\psi_u) \mathcal{A}(u) \begin{bmatrix} \cos(2(\psi_u))E'(u) + \sin(2(\psi_u))B'(u); \end{bmatrix} \quad (23)$$

$$V_{U^0} = f(\psi_u) \mathcal{A}(u) \begin{bmatrix} \sin(2(\psi_u))E'(u) + \cos(2(\psi_u))B'(u); \end{bmatrix} \quad (24)$$

$$V_{RL} = f(\psi_u) \mathcal{A}(u) e^{i2(\psi_u)} (E'(u) + iB'(u)); \quad (25)$$

$$V_{LR} = f(\psi_u) \mathcal{A}(u) e^{i2(\psi_u)} (E'(u) - iB'(u)); \quad (26)$$

As seen in Eq. 25 and 26, the measurement of V_{RL} and V_{LR} measures E and B mode equally, independent of the polarizer rotation. From Eq. 23 and 24, it is seen that V_{Q^0} and V_{U^0} gets unequal contribution from E and B mode, when the baseline and the polarizer frame are aligned as follows:

$$\begin{aligned} V_{Q^0} \quad f(\psi_u) \mathcal{A}(u) E'(u) &: \psi_u \\ f(\psi_u) \mathcal{A}(u) B'(u) &: \psi_u + \pi/4 \\ V_{U^0} \quad f(\psi_u) \mathcal{A}(u) B'(u) &: \psi_u \\ f(\psi_u) \mathcal{A}(u) E'(u) &: \psi_u + \pi/4 \end{aligned}$$

Physically, ψ_u corresponds to aligning x axis of the polarizer frame with the baseline, and $\psi_u + \pi/4$ is rotating the x axis of the polarizer frame from the baseline by 45 on the aperture plane. Compared with those of V_{RL} and V_{LR} in those configuration, either E or B mode in V_{Q^0} and V_{U^0} is suppressed while the other mode is intact. The complete separation of E mode from B mode is not possible unless a full-sky mapping made with infinite angular resolution (Bunn et al. 2003). The leak from E mode into much weaker B mode causes serious problem. We can reduce E mode leak into B mode by measuring V_{Q^0} with $\psi_u + \pi/4$ and V_{U^0} with ψ_u , in which E mode contribution is suppressed.

We have computed the 2x2 leakage matrix (Tegmark 2001) for the simulated observation in x5. L_{EB} indicates the B mode leakage into E mode measurement and L_{BE} indicates the E mode leakage into B mode measurement. If

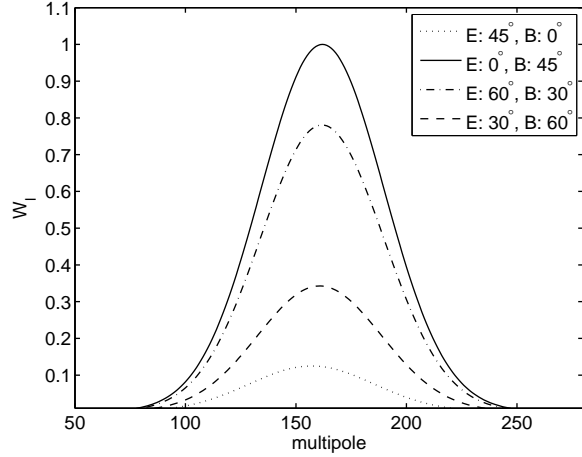


Figure 3. Window functions in V_{Q^0} measurement with 3:4 FWHM

$L_{EB} = L_{BE} = 0$, there is no leakage at all (Tegmark 2001). L_{EB} and L_{BE} are shown for various ψ_u in Fig. 2, where L_{EB} and L_{BE} are dimensionless, and visually identical. It shows that the leakage in V_{Q^0} (V_{U^0}) is smallest at $\psi_u + \pi/4$ (ψ_u). It is seen that with the choice of ψ_u , the leakage of V_{Q^0} and V_{U^0} can be as low as 23% of that of V_{RL} and V_{LR} .

5 VARIATION OF 1- ERROR

It has become standard to estimate band power spectra (Knox 1999) by maximum likelihood method from CMB interferometric observations (Hobson and Masinger 2002). With the Gaussianity of polarimetric visibility and noise, likelihood function is given by

$$L = \frac{1}{(2\pi)^{\frac{N}{2}} \mathcal{J} + N \mathcal{J}^2} \exp[-\frac{1}{2} (S + N)^{-1} \mathcal{J}];$$

where \mathcal{J} is data, S is signal covariance matrix and N is noise covariance matrix. By exploring parameter space to maximize likelihood, we can estimate parameters within certain error limits. The diagonal element of $\mathcal{C}S = \mathcal{C}C_1$, where C_1 is the angular power spectrum, shows the sensitivity of the experiment over multipoles. Through this paper, a window function means $W_l = \mathcal{C}S = \mathcal{C}C_1$. In Appendix A, we have shown analytically that the diagonal W_l^{BB} of V_{Q^0} is maximized at $\psi_u + \pi/4$ while that of V_{U^0} is maximized at ψ_u ; $\psi_u = 2$. We have numerically computed W_l^{EE} and W_l^{BB} for an interferometer of a 25 cm baseline with 30-31 GHz signal frequency range and 3:4 Full Width at Half Maximum (FWHM) beam. They are shown in Fig. 3 and 4, and agree with the analytical result in Appendix A. The window functions are normalized so that the peak value of the highest window function is a unit value. As also shown in Fig. 3 and 4, an interferometer is sensitive to the multipole range $l \sim 2\psi_u \sim 2l$, where ψ_u is a baseline length divided by wavelength and l is FWHM of the window function (for a circular Gaussian beam, $l = 4\sqrt{2} \ln 2 = \text{FWHM}$). In maximum likelihood estimation, it is usual to estimate the band powers (Knox 1999), which are assumed to be at oversome

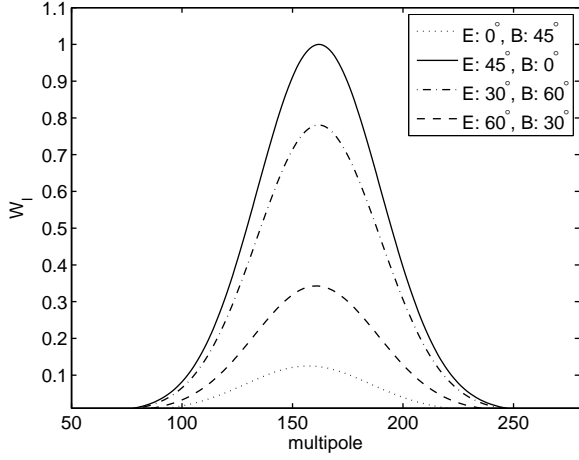


Figure 4. Window functions in V_{Q0} measurement with 3:4 FWHM

multipole range. In an interferometer experiment, E and B mode band power, Δ_{EE} and Δ_{BB} are assumed to be flat over the multipole range the interferometer is sensitive to.

The minimum possible variance on the parameter estimation can be forecast from the Fisher matrix (Dodelson 2003), which is defined as

$$F_{ij} = h \frac{\partial^2 (\ln L)}{\partial \theta_i \partial \theta_j} \quad (27)$$

$$= \frac{1}{2} \text{Tr} \left[\frac{\partial (S+N)}{\partial \theta_i} (S+N)^{-1} \frac{\partial (S+N)}{\partial \theta_j} (S+N)^{-1} \right]$$

Evaluated at the maximum of the likelihood, the square root of diagonal element of the inverse Fisher matrix yields the marginalized 1- σ error on the parameter estimation. As shown analytically in appendix A and numerically in Fig. 3 and 4, diagonal window functions of V_{Q0} and V_{U0} are maximized at certain u . Therefore, Δ_{EE} and Δ_{BB} are expected to be smallest with certain u . We have numerically computed Δ_{EE} and Δ_{BB} from simulated experiments for various u , which are shown in Fig. 5 and 6. In the simulation, we used the CAMB (Lewis et al. 2000) to compute the power spectra of Λ CDM with the tensor-to-scalar ratio ($r = 0.3$). The baseline length 25 [km] is assumed with the signal frequency range 30–31 GHz with 1 GHz bandwidth so that the interferometer probes the multipole range of roughly E1/B1 band of DASI (Kovach et al. 2002). The noise covariance matrix is assumed to be diagonal (White et al. 1999) and have a uniform value, for which we assumed the sensitivity of DASI: $60 \mu\text{Jy s}^{-1/2} \text{m}^{-2}$ (Pryke et al. 2002). We assumed the probe of three fields, thirty six days integration time for each field and simultaneous thirty six orientations for each baseline length. The equatorial coordinates of the assumed three fields are $(80, 0)$, $(80, 120)$ and $(80, 240)$. Fig. 5 and 6 shows Δ_{EE} and Δ_{BB} for various u . To be compared with the CAMB power spectra, Δ_{EE} and Δ_{BB} should be multiplied with $l(l+1) = (2l)$, where $l = 162$ is the multipole our assumed interferometer is most sensitive over. As shown in Fig. 6 that Δ_{BB} is minimum at $u + \pi/4$ in V_{Q0} measurement and at u in V_{U0}

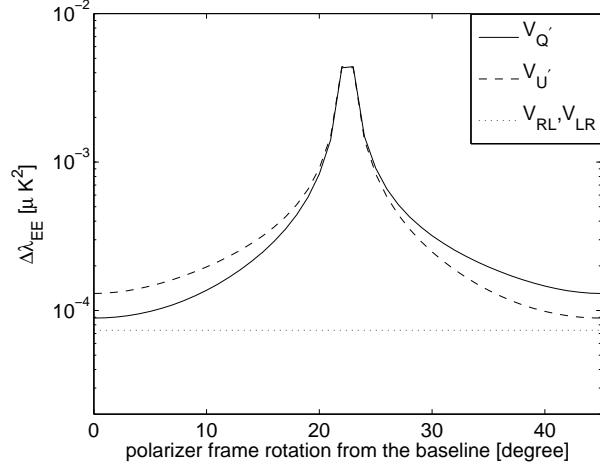


Figure 5. Δ_{EE} for various u

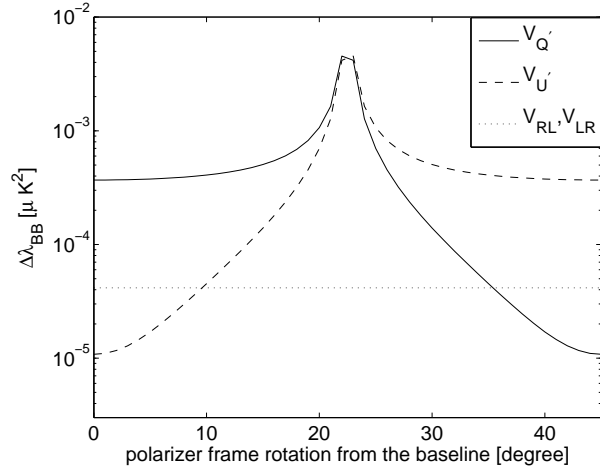


Figure 6. Δ_{BB} for various u

measurement. Δ_{EE} and Δ_{BB} from V_{RL} or V_{LR} are invariant under the rotation of the polarizer frame. For the same assumed noise variance, the minimum Δ_{BB} from V_{Q0} or V_{U0} is 26% of Δ_{BB} from V_{RL} or V_{LR} . It is shown in Fig. 5 that Δ_{EE} is minimum at u in V_{Q0} measurement and at $u + \pi/4$ in V_{U0} measurement. The minimum Δ_{EE} from V_{Q0} or V_{U0} is 1.2 times bigger than the Δ_{EE} from V_{RL} or V_{LR} . V_{RL} and V_{LR} have information on both of Q^0 and U^0 , while V_{Q0} and V_{U0} have information on either of Q^0 and U^0 . It may seem odd that Δ_{BB} of V_{Q0} and V_{U0} can be smaller than Δ_{BB} of V_{RL} and V_{LR} , though more information are contained in V_{RL} and V_{LR} . Δ_{BB} is the estimation error marginalized over Δ_{EE} , since the likelihood in the simulated observation is the function of two parameters, Δ_{EE} and Δ_{BB} . Δ_{BB} is given by $\frac{\partial L_B}{\partial \Delta_{BB}} = 0$, where

$$\frac{\partial L_B}{\partial \Delta_{BB}} = 0; \quad \frac{L_B(\frac{1}{\Delta_{BB}})}{L_B(\frac{0}{\Delta_{BB}})} = e^{1-2}$$

6 Jaiseung Kim

$L_B (B_B)$, which is the likelihood function marginalized over E mode band power, is as follows:

$$L_B (B_B) = \int d_{EE} L (EE; BB; EB = 0):$$

$L (EE; BB)$ becomes less sensitive to the variation of E_{EE} with reduced contribution of E mode to visibilities. It makes the $L_B (B_B)$ more sharply peaked around $\hat{0}_{BB}$, which leads to the reduction of B_B .

The 1- error on power spectra estimation is the sum of sample variance and noise variance (Park et al. 2003):

$C_1 - C_1 = (2l + 1) + N$, where N is noise variance. In the case of circular polarizers, B_B is smaller than E_{EE} due to the smaller sample variance of B mode than that of E mode, even though visibilities with circular polarizers have equal sensitivity to both E and B mode.

6 FEEDHORN ARRAY

For optimization, the polarizer frame should be oriented with certain rotation from all the baselines formed by the feedhorn the polarizer is associated with. When there are just two feedhorns, there is a single baseline and orienting the polarizer frame to specific rotation physically is trivial. But in most of real CMB experiments, an array consisting of more than two feedhorns are employed. When all the feedhorns (apertures) are aligned on a straight line, orienting polarizers with specific rotation from all the associated baselines is also trivial even for a ($N > 2$) feedhorn array. When the feedhorn array is configured on some two dimensional pattern for the optimal uv coverage (Guyon and Roddier 2001; Pryke et al. 2002), it is not possible to realize specific rotation of the polarizer frame from all the associated baselines. We can achieve the optimal polarizer rotation for a array of multiple feedhorns ($N > 2$) by forming certain linear combination of visibilities as follows. With the employment of orthomode transducer (OMT), each baseline measures the real and imaginary part of V_{Q0} and V_{U0} respectively. Four measured values are obtained such that $V_1 = \text{Re}[V_{Q0}]$, $V_2 = \text{Im}[V_{Q0}]$, $V_3 = \text{Re}[V_{U0}]$, $V_4 = \text{Im}[V_{U0}]$. With Eq. 9 and 10, V_1, V_2, V_3 , and V_4 are as follows:

$$V_1 = f(\hat{n}) \int dA(\hat{n}, \hat{n}_A) \quad (28)$$

$$\text{Re} \int_Z e^{i(2 - 2)(\hat{n})} (Q(\hat{n}) + iU(\hat{n})) \cos(2u - \hat{n})$$

$$V_2 = f(\hat{n}) \int dA(\hat{n}, \hat{n}_A) \quad (29)$$

$$\text{Re} \int_Z e^{i(2 - 2)(\hat{n})} (Q(\hat{n}) + iU(\hat{n})) \sin(2u - \hat{n});$$

$$V_3 = f(\hat{n}) \int dA(\hat{n}, \hat{n}_A) \quad (30)$$

$$\text{Im} \int_Z e^{i(2 - 2)(\hat{n})} (Q(\hat{n}) + iU(\hat{n})) \cos(2u - \hat{n});$$

$$V_4 = f(\hat{n}) \int dA(\hat{n}, \hat{n}_A) \quad (31)$$

$$\text{Im} \int_Z e^{i(2 - 2)(\hat{n})} (Q(\hat{n}) + iU(\hat{n})) \sin(2u - \hat{n}):$$

With these, we can form two linear combinations V_E and V_B such that

$$V_E = \text{Re} \int_Z e^{i(2 - 2)(\hat{n})} (V_1 + iV_3) + i \text{Re} \int_Z e^{i(2 - 2)(\hat{n})} (V_2 + iV_4);$$

$$V_B =$$

$$\text{Im} \int_Z e^{i(2 - 2)(\hat{n})} (V_1 + iV_3) + i \text{Im} \int_Z e^{i(2 - 2)(\hat{n})} (V_2 + iV_4);$$

With Eq. 28, 29, 30 and 31, we can easily show that

$$V_E = f(\hat{n}) \int dA(\hat{n}, \hat{n}_A)$$

$$\text{Re} \int_Z e^{i(2 - 2)(\hat{n})} (Q(\hat{n}) + iU(\hat{n})) e^{i2u - \hat{n}}$$

$$V_B = f(\hat{n}) \int dA(\hat{n}, \hat{n}_A)$$

$$\text{Im} \int_Z e^{i(2 - 2)(\hat{n})} (Q(\hat{n}) + iU(\hat{n})) e^{i2u - \hat{n}};$$

We can identify the linear combination V_E with the V_{Q0} and V_B with the V_{U0} , whose polarizer frame is aligned with the associated baseline. Hence, the linear combination V_E is optimized for E mode measurement and V_B is for B mode measurement. Linear combination V_E and V_B enable the optimization for a array of multiple feedhorns ($N > 2$).

7 CONCLUSION

As shown in this paper, the contribution from E and B mode to V_{Q0} and V_{U0} are variant under the rotation of the polarizer frame. In appendix A, we have shown analytically that the diagonal window functions of V_{Q0} and V_{U0} are maximized, when x axis of the polarizer frame is rotated from the associated baseline with certain angles. The 1- error on power spectra estimation from V_{Q0} and V_{U0} measurement are also variant under the rotation of the polarizer frame. Huge variation of 1- error are shown in the simulated observation of the configuration similar to the DASI. The 1- error on B mode power spectrum estimation is minimized, when x axis of polarizers is rotated from the baseline by 45 in V_{Q0} measurement (when x axis of polarizers is aligned with the baseline in V_{U0} measurement). Simulation shows that minimum 1- error on B mode power spectra estimation in V_{Q0} or V_{U0} is 26% of that from V_{RL} or V_{LR} , though more information are measured in V_{RL} or V_{LR} . The simulation also shows that the E/B mixing in V_{Q0} or V_{U0} can be as low as 23% of that in V_{RL} or V_{LR} . With choice of polarizer rotation from the baseline, we can achieve B mode sensitivity and E/B separability from V_{Q0} or V_{U0} measurement several times better than V_{RL} or V_{LR} measurement in the same configuration.

For a array of multiple feedhorns ($N > 2$), there always exist certain linear combinations of visibilities, which are equivalent to visibilities of the optimal polarizer rotation. B mode optimization can be achieved for a feedhorn array ($N > 2$) by forming the linear combinations.

With integration time which makes the noise variance equal to the sample variance, the estimation error on the power spectra is minimized (Bowden et al. 2004; Park et al. 2003). In parallel with the choice for the polarizer rotation from the baseline, we can optimize the interferometer for B mode with the integration time which makes the sample variance of B mode equal to the noise variance.

8 ACKNOWLEDGMENTS

The author thanks Gregory Tucker, Peter Timbie, Emory Bunn, Andrei Korotkov and Carolina Calderon for useful

discussions. He thanks Douglas Scott for the hospitality during the visit to UBC. He thanks anonymous referees for thorough reading and helpful comments, which led to significant improvements in the paper.

REFERENCES

- Arfken G. B. and Weber H. J., *Mathematical Methods for Physicists*. Elsevier Science & Technology Books, 5th edition, 2000.
- Bowden M. et al., *Mon. Not. R. Astron. Soc.*, 349, 321, 2004.
- Bunn E. F., Zaldarriaga M., Tegmark M., and de Oliveira-Costa A., *Phys. Rev. D*, 67, 2003.
- Dodelson S., *Modern Cosmology*. Academic Press, 2nd edition, 2003.
- Guyon O. and Roddier F., *PASP*, 113, 98, 2001.
- Hobson M. and Muisinger K., *Mon. Not. R. Astron. Soc.*, 334, 569, 2002.
- Kamionkowski M., Kosowsky A., and Stebbins A., *Phys. Rev. D*, 55, 7368, 1997.
- Knox L., *Phys. Rev. D*, 60, 1999.
- Korotkov A. et al., In J. Zmuidzinas, W. S. Holland, S. Whittington, and W. D. Duncan, editors, *Millimeter and Submillimeter Detectors and Instrumentation for Astronomy III*, volume 6275, 2006.
- Kovac J., *Nature*, 420, 772, 2002.
- Kraus J., *Radio Astronomy*. Cygnus-Quasar Books, 2nd edition, 1986.
- Lawson P., eds, *Principles of Long Baseline Stellar Interferometry*. 1999 Michelson Summer School, 1999.
- Lewis A., Challinor A., and Lasenby A., *Astrophys. J.*, 538, 473, 2000. <http://cambridge.org/>.
- Hobson M. P. and Muisinger K., *Mon. Not. R. Astron. Soc.*, 334, 569, 2002.
- Okamoto T. and Hu W., *Phys. Rev. D*, 67, 2003.
- Page L. et al., submitted *ApJ*, 2006.
- Park C.-G. et al., *Astrophys. J.*, 589, 67, 2003.
- Pryke C., *Astrophys. J.*, 568, 28, 2002.
- Seljak U. and Zaldarriaga M., *Phys. Rev. Lett.*, 78, 2054, 1997.
- Tegmark M., *Phys. Rev. D*, 64, 2001.
- Tucker G. S. et al., *New Astronomy Reviews*, 47, 1173-1176, 2003.
- White M. et al., *Astrophys. J.*, 514, 12, 1999.
- White M. and Srednicki M., *Astrophys. J.*, 443, 6, 1995.
- Zaldarriaga M., *Astrophys. J.*, 503, 1, 1998.
- Zaldarriaga M. and Seljak U., *Phys. Rev. D*, 55, 1830, 1997.

APPENDIX A: WINDOW FUNCTIONS

A1 flat sky approximation in small angle limit

As discussed in §4, visibilities with flat sky approximation are as follows:

$$V_{Q^0} = f(\ell) \int_{\mathcal{D}} d^2 u^0 \tilde{\mathcal{A}}(u, u^0) [\cos(2(\alpha - \alpha^0))E^*(u^0) + \sin(2(\alpha - \alpha^0))B^*(u^0)];$$

$$V_{U^0} = f(\ell) \int_{\mathcal{D}} d^2 u^0 \tilde{\mathcal{A}}(u, u^0) [\sin(2(\alpha - \alpha^0))E^*(u^0) + \cos(2(\alpha - \alpha^0))B^*(u^0)];$$

$$V_{RL} = f(\ell) \int_{\mathcal{D}} d^2 u^0 \tilde{\mathcal{A}}(u, u^0) e^{i2(\alpha - \alpha^0)} (E^*(u^0) + iB^*(u^0));$$

$$V_{LR} = f(\ell) \int_{\mathcal{D}} d^2 u^0 \tilde{\mathcal{A}}(u, u^0) e^{i2(\alpha - \alpha^0)} (E^*(u^0) - iB^*(u^0));$$

For multipole $\ell > 60$, the following relations between the flat sky power spectra and the exact power spectra from spherical sky works within one percent error (White et al. 1999):

$$hE(\ell)E^*(\ell^0) \approx C_1^{EE}(\ell, \ell^0)_{\ell=2}^{\ell^0}; \quad (\text{A1})$$

$$hB(\ell)B^*(\ell^0) \approx C_1^{BB}(\ell, \ell^0)_{\ell=2}^{\ell^0}; \quad (\text{A2})$$

$$hE(\ell)B^*(\ell^0) \approx 0; \quad (\text{A3})$$

With the correspondence of the power spectra between flat sky and spherical sky, it can be easily derived that diagonal elements of E/B window functions and their derivatives with respect to the rotation of the polarizer frame, α , are as follows:

$$(i) hV_{Q^0}(\ell)V_{Q^0}^*(\ell^0) \approx$$

$$W^{EE}(\ell; \ell^0) = \int_{\mathcal{D}} f^2(\ell) u^0 \cos^2(2(\alpha - \alpha^0)) \tilde{\mathcal{A}}(u, u^0) \tilde{\mathcal{A}}^*(u, u^0) d_{u^0};$$

$$W^{BB}(\ell; \ell^0) = \int_{\mathcal{D}} f^2(\ell) u^0 \sin^2(2(\alpha - \alpha^0)) \tilde{\mathcal{A}}(u, u^0) \tilde{\mathcal{A}}^*(u, u^0) d_{u^0};$$

$$\frac{\partial W^{EE}(\ell; \ell^0)}{\partial \alpha} = f^2(\ell) u^0 \int_{\mathcal{D}} d_{u^0} \tilde{\mathcal{A}}^2(u, u^0) [2 \sin 4(\alpha - \alpha^0) \cos 4(\alpha - \alpha^0) + 2 \cos 4(\alpha - \alpha^0) \sin 4(\alpha - \alpha^0)];$$

$$\frac{\partial W^{BB}(\ell; \ell^0)}{\partial \alpha} = f^2(\ell) u^0 \int_{\mathcal{D}} d_{u^0} \tilde{\mathcal{A}}^2(u, u^0) [2 \sin 4(\alpha - \alpha^0) \cos 4(\alpha - \alpha^0) - 2 \cos 4(\alpha - \alpha^0) \sin 4(\alpha - \alpha^0)];$$

$$(ii) hV_{U^0}(\ell)V_{U^0}^*(\ell^0) \approx$$

$$W^{EE}(\ell; \ell^0) = \int_{\mathcal{D}} f^2(\ell) u^0 \sin^2(2(\alpha - \alpha^0)) \tilde{\mathcal{A}}(u, u^0) \tilde{\mathcal{A}}^*(u, u^0) d_{u^0};$$

$$W^{BB}(\ell; \ell^0) = \int_{\mathcal{D}} f^2(\ell) u^0 \cos^2(2(\alpha - \alpha^0)) \tilde{\mathcal{A}}(u, u^0) \tilde{\mathcal{A}}^*(u, u^0) d_{u^0};$$

$$\frac{\partial W^{EE}(\ell; \ell^0)}{\partial \alpha} = f^2(\ell) u^0 \int_{\mathcal{D}} d_{u^0} \tilde{\mathcal{A}}^2(u, u^0) [2 \sin 4(\alpha - \alpha^0) \cos 4(\alpha - \alpha^0) - 2 \cos 4(\alpha - \alpha^0) \sin 4(\alpha - \alpha^0)];$$

$$\frac{\partial W^{BB}(\ell; \ell^0)}{\partial \alpha} = f^2(\ell) u^0 \int_{\mathcal{D}} d_{u^0} \tilde{\mathcal{A}}^2(u, u^0)$$

$$[2 \sin^4 \alpha \cos^4 \alpha + 2 \cos^4 \alpha \sin^4 \alpha]$$

(iii) $h_{V_{RL}}(u)V_{RL}(u)$ and $h_{V_{LR}}(u)V_{LR}(u)$,

$$W^{EE}(u;u^0) = W^{BB}(u;u^0) =$$

$$f^2(\alpha)u^0 \tilde{A}(u-u^0)\tilde{A}(u+u^0)d\alpha;$$

$$\frac{\partial W^{EE}(u;u^0)}{\partial \alpha} = \frac{\partial W^{BB}(u;u^0)}{\partial \alpha} = 0;$$

From (iii), we can see that the diagonal E and B mode window functions in V_{RL} and V_{LR} measurement are invariant under the rotation of the polarizer frame. From (i) and (ii), we can see that the derivatives of the diagonal E/B window functions in V_{Q^0} and V_{U^0} measurement are zero, when

$$\sin^4 \alpha \frac{d}{d\alpha} \tilde{A}^2(u-u^0) \cos^4 \alpha + \cos^4 \alpha \frac{d}{d\alpha} \tilde{A}^2(u+u^0) \sin^4 \alpha = 0, \quad (A4)$$

, which satisfies Eq. A4, is

$$= \frac{1}{4} \tan^{-1} \frac{R \frac{d}{d\alpha} \sin^4 \alpha \tilde{A}^2(u-u^0)}{d \cos^4 \alpha \tilde{A}^2(u+u^0)} : \quad (A5)$$

A Gaussian beam is a good approximation to many CMB experiments and the Fourier transform of a Gaussian beam is

$$\tilde{A}(u-u^0) = \exp\left[-\frac{j(u-u^0)^2}{2}\right] \\ = \exp\left[-\frac{[u^2 + u^{02} - 2uu^0 \cos(\alpha - \alpha^0)]^2}{2}\right];$$

where $\alpha = 0.4245$ FWHM. With a Gaussian beam, the argument of \tan^{-1} in Eq. A5 is

$$\frac{R_2 \frac{d}{d\alpha} \sin^4 \alpha \exp[2uu^0 \cos(\alpha - \alpha^0)]}{R_2 \frac{d}{d\alpha} \cos^4 \alpha \exp[2uu^0 \cos(\alpha + \alpha^0)]} \\ = \frac{R_2 \frac{d}{d\alpha} \sin^4(\alpha + \alpha^0) \exp[2uu^0 \cos(\alpha - \alpha^0)]}{R_2 \frac{d}{d\alpha} \cos^4(\alpha + \alpha^0) \exp[2uu^0 \cos(\alpha + \alpha^0)]} \\ = \frac{R_2 \frac{d}{d\alpha} \sin^4(\alpha + \alpha^0) \exp[2uu^0 \cos(\alpha - \alpha^0)]}{R_2 \frac{d}{d\alpha} \cos^4(\alpha + \alpha^0) \exp[2uu^0 \cos(\alpha + \alpha^0)]} \\ = \frac{\sin^4 \alpha \frac{d}{d\alpha} \cos^4 \alpha \exp[2uu^0 \cos(\alpha - \alpha^0)]}{\cos^4 \alpha \frac{d}{d\alpha} \sin^4 \alpha \exp[2uu^0 \cos(\alpha + \alpha^0)]} \\ = \tan^4 \alpha \quad (A6)$$

From the third line to the fourth line in Eq. A6, $\frac{R_2}{d} \frac{d}{d\alpha} \sin^4 \alpha \exp[2uu^0 \cos(\alpha - \alpha^0)] = 0$ was used. By plugging Eq. A6 into Eq. A5, we get

$$= \frac{1}{4} \tan^{-1}(\tan^4 \alpha) \\ = \frac{n}{4} \quad (n = \dots; 2; 1; 0; 1; 2; \dots);$$

where α is the orientation of the baseline. The diagonal element of E and B mode window functions of V_{Q^0} and V_{U^0} is extremized, when x axis of the polarizer is in rotation from the baseline by $90^\circ, 45^\circ, 0^\circ, 45^\circ, 90^\circ$. Since the second

derivative of diagonal element of E mode window function has the opposite sign of that of B mode window function, the diagonal element of B mode window function is minimized at the polarizer rotation which maximizes the diagonal element of E mode window function, and vice versa.

A.2 spherical sky

Visibilities from spherical sky are as follows:

$$V_{Q^0} = \frac{1}{2} f(\alpha) \int_{\mathcal{Z}} dA(\hat{n}; \hat{n}_A) e^{i(2u-\hat{n})} \quad (A7)$$

$$[e^{i(2-\hat{n})} (a_{E;l,m} + ia_{B;l,m}) {}_2Y_{lm} \\ + e^{i(2+\hat{n})} (a_{E;l,m} - ia_{B;l,m}) {}_2Y_{lm}]$$

$$V_{U^0} = \frac{i}{2} f(\alpha) \int_{\mathcal{Z}} dA(\hat{n}; \hat{n}_A) e^{i(2u-\hat{n})} \quad (A8)$$

$$[e^{i(2-\hat{n})} (a_{E;l,m} + ia_{B;l,m}) {}_2Y_{lm} \\ - e^{i(2+\hat{n})} (a_{E;l,m} - ia_{B;l,m}) {}_2Y_{lm}]$$

$$V_{RL} = f(\alpha) \int_{\mathcal{Z}} dA(\hat{n}; \hat{n}_A) \quad (A9)$$

$$(a_{E;l,m} + ia_{B;l,m}) {}_2Y_{lm} e^{i(2u-\hat{n}^2+2\hat{n})};$$

$$V_{LR} = f(\alpha) \int_{\mathcal{Z}} dA(\hat{n}; \hat{n}_A) \quad (A10)$$

$$(a_{E;l,m} - ia_{B;l,m}) {}_2Y_{lm} e^{i(2u-\hat{n}^2-2\hat{n})};$$

With Eq. A7, A8, A9, and A10, visibilities from spherical sky can be expressed as follows:

$$V_{Q^0}(\hat{n}; u) = \sum_{l,m} (e^{i2R_{lm}} + e^{i2L_{lm}}) a_{E;l,m} \\ + i \sum_{l,m} (e^{i2R_{lm}} - e^{i2L_{lm}}) a_{B;l,m}; \quad (A11)$$

$$V_{U^0}(\hat{n}; u) = \sum_{l,m} i(e^{i2R_{lm}} - e^{i2L_{lm}}) a_{E;l,m} \\ + \sum_{l,m} (e^{i2R_{lm}} + e^{i2L_{lm}}) a_{B;l,m}; \quad (A12)$$

$$V_{RL}(\hat{n}; u) = \sum_{l,m} 2(a_{E;l,m} + ia_{B;l,m}) e^{i2R_{lm}}; \quad (A13)$$

$$V_{LR}(\hat{n}; u) = \sum_{l,m} 2(a_{E;l,m} - ia_{B;l,m}) e^{i2L_{lm}}; \quad (A14)$$

where

$$R_{lm} = \frac{f(\alpha)}{2} \int_{\mathcal{Z}} dA(\hat{n}; \hat{n}_A) {}_2Y_{lm} e^{i(2u_i - \hat{n}^2 + 2\hat{n})};$$

$$L_{lm} = \frac{f(\alpha)}{2} \int_{\mathcal{Z}} dA(\hat{n}; \hat{n}_A) {}_2Y_{lm} e^{i(2u_i - \hat{n}^2 - 2\hat{n})};$$

and \hat{n}_A indicates the direction of antenna pointing.

Spin-2 spherical harmonics have the following form (Zaldarriaga 1998).

$${}_2Y_{lm}(\hat{n}) = \frac{r}{4} (F_{1;l,m}(\alpha) + F_{2;l,m}(\alpha)) e^{im};$$

$${}_2Y_{lm}(\hat{n}) = \frac{r}{4} (F_{1;l,m}(\alpha) - F_{2;l,m}(\alpha)) e^{im};$$

where $F_{1;l,m}$ and $F_{2;l,m}$ can be computed in terms of Legendre

10 Jaiseung Kim

$$= e^{i\frac{1}{2}(m-2)\theta} e^{i(m-2)\theta} u_{2,lm}; \quad (A 18)$$

where

$$u_{2,lm} = \frac{r}{Z} \frac{(2l+1)}{4} \int_0^{\pi} d\theta \sin(\theta) A(\theta) J_{m+2}(2u \sin(\theta)) (F_{1,lm}(\theta) + F_{2,lm}(\theta));$$

$$u_{2,lm} = \frac{r}{Z} \frac{(2l+1)}{4} \int_0^{\pi} d\theta \sin(\theta) A(\theta) J_{m-2}(2u \sin(\theta)) (F_{1,lm}(\theta) - F_{2,lm}(\theta));$$

By plugging Eq. A 17 and A 18 into Eq. A 16, we get

$$= \frac{1}{4} \tan^{-1} \frac{\text{Im} [R_{i,lm} L_{i,lm}]}{\text{Re} [R_{i,lm} L_{i,lm}]}$$

$$= \frac{1}{4} \tan^{-1} \frac{\text{Im} [e^{i4\theta} u]_{lm-2,lm}}{\text{Re} [e^{i4\theta} u]_{lm-2,lm}}$$

$$= u + \frac{n}{4}; \quad (n = \dots; 2; 1; 0; 1; 2; \dots)$$

$= u + \frac{n}{4}$ extremize the diagonal element of E and B mode window functions of V_{Q0} and V_{U0} , which is consistent with the result obtained with θ at sky approximation.